Alexandria Engineering Journal (2012) 51, 95–107

Alexandria University

Alexandria Engineering Journal

www.elsevier.com/locate/aej
www.sciencedirect.com

Behavior of portal frames of steel hollow sections exposed to fire

Mohamed Mahmoud El-Heweity

Structural Engineering Department, Faculty of Engineering, Alexandria University, Egypt

Received 21 May 2012; revised 12 June 2012; accepted 25 June 2012
Available online 13 September 2012

KEYWORDS

Fire load;
Portal frames;
Steel hollow sections;
Failure mechanisms;
Non-linearity and numerical analysis

Abstract This paper presents a numerical study concerning the behavior of hollow sections steel portal frames exposed to fire. A model is developed to employ both thermal and structural responses incorporating material and geometric non-linearities. To establish the failure mechanism of a frame under fire conditions, a failure criterion is proposed and validated against available experimental data. The failure temperatures predicted through the suggested failure criterion show good agreement compared to the experimental results. A parametric study is then conducted using the calibrated model to focus on failure mechanisms and associated failure temperatures. Variables considered are fire condition and rafter's inclination angle. The assessment of frame performance is based on the generated failure mechanism and enhancement of failure temperature due to the chosen parameters. Results indicate that the studied variables strongly affect the failure mechanisms of portal frames. Contradictory, their effects on the failure temperature are minimal. Finally, the study presents vital outlines for the designer to find out and hence trace the failure mechanism prior to the completion of the final design stage. Only at this point, the optimum fire protection or adequate section capacity can be accomplished and may seriously be implemented in the field of industrial steel constructions.

1. Introduction

Portal frame construction is one of the most common structural systems used in industrial single story buildings. A number of recent fires in industrial warehouses have drawn attention to a current lack of understanding about the structural response of portal frames under elevated temperatures. One of the major disadvantages of steel constructions is its sensitivity to fire, as steel looses strength and stiffness rapidly. Thus, fire protection is often requires, which can add to the expense of construction. The behavior of steel members during fire is complex and very much dependent on the restraint at the member ends. The restraint at member ends depends mainly on the rigidity of the joints connecting the members and the stiffness provided by the adjacent members [1].

The behavior of steel members subjected to realistic fire conditions is quite difficult and expensive. Natural fire tests, such as the Cardington tests [2], are ideal as they reproduce reality very closely but it is quite difficult to obtain detailed

E-mail address: ugss_alexandria@yahoo.com

Peer review under responsibility of Faculty of Engineering, Alexandria University.

Production and hosting by Elsevier

1110-0168 © 2012 Faculty of Engineering, Alexandria University. Production and hosting by Elsevier B.V. All rights reserved.
http://dx.doi.org/10.1016/j.aej.2012.06.004

measurements of the mechanical response of individual members and to quantify the various parameters that control their behavior. Thus, the development of such numerical tools is necessary for applications as the use of fire tests is limited due to the high cost associated with the tests. These numerical tools are formulated mostly through the finite-element method by Schleich et al. [3], Saab and Nethercot [4], Liu [5], Najjar and Burgess [6], and Morris and Kirby [7].

On the other hand, most design codes allow simplified methods that provide simple procedures with empirical formulae for conducting analysis of structures under fire conditions. However, these simplified procedures usually make convenient assumptions that may result in conservative solutions [8]. A major concern is the effects of the load redistribution capability and continuity of the structural members which is completely ignored by simple procedures. Fire tests conducted by O'Connor and Martin [9] indicated that structural steel members in steelwork behave significantly better than single members with isolated restraining conditions. In fact, for structural integrity, the main aim is to prevent the temperatures in the structure from reaching a critical level within a specified period of time beyond which the structure may collapse. If the temperature–time relationship for a specific fire environment is known, perhaps through some heat transfer calculations, the problem then remaining is to establish the relationship between rising temperature and structural behavior until collapse [8].

Recently, many research works were conducted on the behavior of steel frames whether these frames are portal, single-story, multi-story, pitched roof and multi-bays. El-heweity [10] studied the effect of the frame action on the behavior of steel rafters exposed to fire. Wong [11] studied the responses of industrial pitched portal frame structures in fire both experimentally and numerically. He developed an approach for calculating the critical temperature of a steel portal frame. Song et al. [12] also performed a study on the behavior of portal frames using dynamic analysis to investigate the failure mechanism of a single story haunched portal frame in fire subjected to different support conditions at their column base. However, Yin and Wang [13] performed a numerical study of large deflection behavior of restrained steel rafters at elevated temperatures. They established that the large deflection behavior of steel rafters could significantly affect their survival temperature in fire. On the other hand, Rahman et al. [14] studied the overturning moments of portal frames at elevated temperatures. In their analyses, they predicted the post-snap-through-buckling behavior of portal frames.

2. Scope

Failure is among the interest of assessing the behavior of steel portal frames subjected to fire loads. In such cases, failure criterion is still a matter of arguments among researchers especially for frames with steel hollow sections. From general prospective, it is believed that selecting the appropriate criterion is of great importance to evaluate the behavior of frames under different fire conditions. This point is directly addressed in the current research. This paper provides investigation of this subject using a powerful finite-element software package 'SAFIR' [15]. The study focuses on the straining actions, deformations and stresses affecting the failure behavior of portal frame assembly. The work provides useful information about both failure mechanism and failure temperature as affected by fire conditions and the rafter's inclination angle as well. The evaluation of the chosen variables is explored. The work concludes failure criterion-based guidelines that may be useful in codes provisions and may seriously be considered for frames subjected to fire loading.

3. Numerical model

3.1. Introduction

In order to study the behavior of the steel portal frame exposed to fire, the software program SAFIR [15] is utilized to analyze the subject frames for both thermal and structural analyses. In the phase of thermal analysis, heat transfer study is conducted to compute the temperature gradients through the cross-sections of the frame members, while the second phase of structural analysis is used to calculate the straining actions of the structural members. The implemented numerical model is detailed in the following sections.

3.2. Material properties at elevated temperatures

The reduction of the mechanical properties of steel at different temperatures as compared to that at ambient temperature is presented in Fig. 1 on the basis of Eurocode 3 criteria [16]. As can be seen, there is no loss in yield strength at temperatures up to 400 °C; however, the elastic modulus starts to fail down from approximately 100 °C. It should be noted that the coefficient of thermal expansion is considered as suggested by Eurocode 3 [16]. Actually, a value of 0.3 is used for Poisson's ratio in the analysis, and steel is considered as an isotropic material with a density of 7850 kg/m^3.

3.3. Finite elements and mesh discretization

The numerical analysis was performed with the finite element program SAFIR [15]. The cross-sections of the steel members are discretized and modeled as rectangular elements while each frame member is divided to five elements. The grids of finite elements are then used to calculate the temperature distribution across each cross section considered.

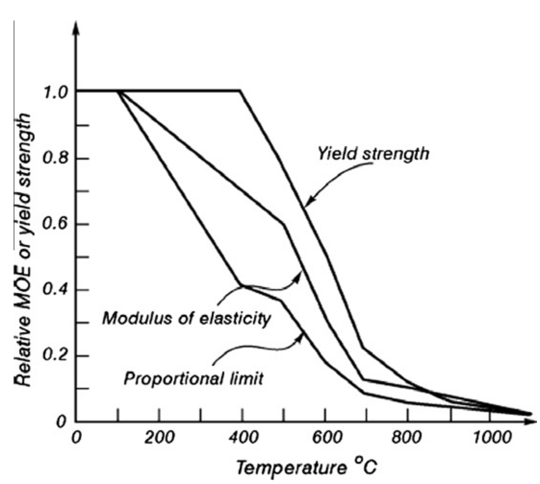

Figure 1 Reduction in steel's yield stress and modulus of elasticity with temperature according to EC3 [16].

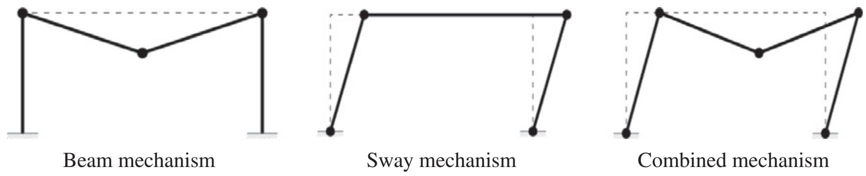

Figure 2 Expected failure mechanisms of horizontal portal frames.

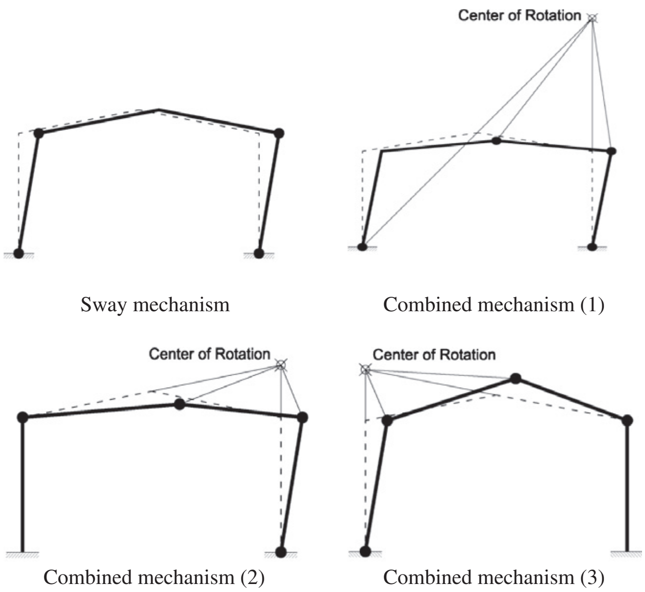

Figure 3 Expected failure mechanisms of pitched roof portal frames.

3.4. Fire load

In the presented model, the fire load is simulated using the standard ISO-834 fire curve [17] which is applied to the surfaces of the structural members exposed to fire as a thermal load. Meanwhile, vertical and/or horizontal loads carried out at ambient temperature is applied and remained constant throughout the analysis.

3.5. Proposed failure criteria

In order to assess the occurrence of failure throughout the fire event, proposing a reliable failure criterion is a must. It is strongly believed herein that adequate failure criterion can be established by assuming that failure occurs when sufficient plastic hinges are attained to create a mechanism. Actually, the formation of plastic hinges is associated with yielding of the cross-section. It should be pointed out that the yield stress of steel is reduced with the presence of the elevated temperature. This definitely reduces the plastic moment capacity of the steel section. Provided sufficient plastic hinges are formed in steel members, it is possible to calculate the failure temperature required to form mechanism. From another prospective, failure mechanisms are changed by changing the geometry of the frame. Generally, three possible mechanisms are traced for horizontal portal frames as shown in Fig. 2. Theses include beam mechanism, sway mechanism or combined mechanism. In addition, for pitched roof portal frames four possible mechanisms can be expected as shown in Fig. 3. It should be noted that the beam mechanism is not expected for pitched roof frames unless it is combined with the formation of any plastic hinge at column. Detailed illustrations may be seen elsewhere [18–20].

4. Model validation

Tests conducted by Rubert and Schaumann [21] are used to validate the proposed model. One of these tests, namely EGR, concerning single-bay simply-supported frame is shown in Fig. 4. Seven test results of EGR frames are considered in which the frames were fully heated. Table 1 summarizes the geometries and loadings of the frames. In the analyses, each steel member was typically divided into five elements. The stress–strain relationship suggested by Rubert and Schaumann [21] is utilized. Elastic modulus of steel at ambient temperature is considered 2×10^5 MPa and all frame sections are assumed to be IPE 80 as considered in Ref. [21].

Table 1 shows a comparative study between the failure temperatures obtained from test results, T_{ftest}, and those predicted by the proposed model, T_{fmodel}. The results show good agreement with an average difference between the predicted and experimental values on the range of 7.4% with a coefficient of variation (COV) of 3.2% indicating the efficiency of the considered failure criteria.

5. Parametric study

In this parametric study, the effects of both fire cases and rafter's inclinations are scrutinized. A portal frame with dimensions illustrated in Fig. 5 is examined. The frame consists of unprotected steel rafter and unprotected and/or protected steel columns. The rafter is connected to the columns with rigid moment resisting rafter-column joints. The columns of the frame are fixed to rigid supports at the bottom. The frame is loaded through a uniformly distributed load of 10 kN/m. This loading

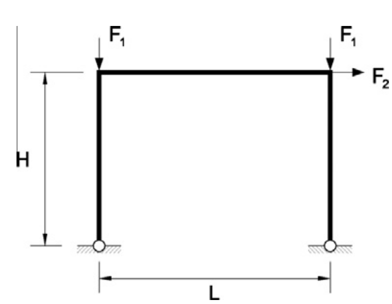

Figure 4 Schematic of frame tested by Rubert and Schaumann [21].

Table 1 Model's Calibration.

Frame designation	Dimensions (mm)		Steel's yield stress	Loads (kN)		T_{fmodel}/T_{ftest}
	L	H		$F1$	$F2$	
EGR1B	1220	1170	382	65	2.5	0.9549
EGR1C	1220	1170	382	65	2.5	0.9689
EGR2	1220	1170	385	40	1.6	0.9314
EGR3	1220	1170	385	77	3.0	0.9356
EGR4	1220	1170	412	77	3.0	0.9175
EGR5	1220	1170	412	88	3.4	0.8806
EGR6	1220	1170	412	88	3.4	0.8914
Mean						0.9258
COV						3.2%

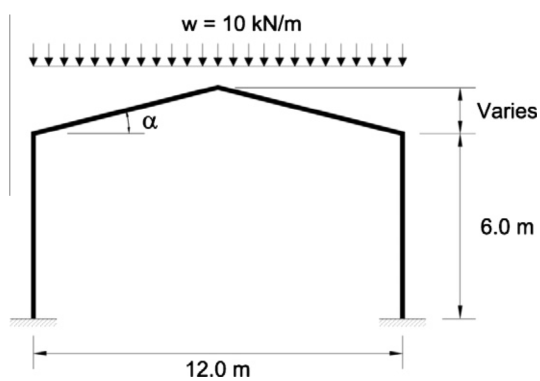

Figure 5 Schematic of analyzed portal frame.

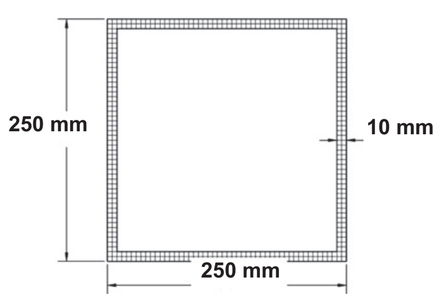

Figure 6 Finite element discretization of the steel hollow section.

was applied at ambient temperature and remained constant throughout the analysis. In addition to the applied loads, the frame is subjected to a fire load which is simulated using the standard ISO-834 fire curve [17] and applied to the surfaces of the structural members exposed to fire as a thermal load.

The frame is designed according to ECP-LRFD [22] design code and all members are comprised of squared steel hollow sections shown in Fig. 6 and detailed in Table 2. The numerical analysis was performed with the finite element program SAFIR [15]. The cross-sections of the steel members are discretized and modeled as rectangular elements. As shown in Fig. 6, the grids of finite elements are then used to calculate the temperature distribution across each cross section considered. The mesh sizes are chosen to be adequate to decrease

Table 2 Cross-sectional dimensions of frame members.

Member	Dimensions and properties of the cross-section				
	b (mm)	h (mm)	t_1 (mm)	A (mm^2)	I (mm^4)
Column	250	250	10	9600	9.23×10^7
Rafter	250	250	10	9600	9.23×10^7

the computational time with 384 elements and 576 nodes. This is matched with the sensitivity analysis on mesh discretization carried out by Welsh [23] who found that using very fine discretized section has little effect on the thermal and structural output.

The material properties of columns and rafter, at ambient temperature, are: yield stress; $f_y = 240$ MPa, modulus of elasticity; $E = 210$ GPa, Poisson's ratio; $v = 0.3$ and shear modulus; $G = 8.4$ GPa.

Lateral geometrical imperfections for columns are considered herein to be 1/1000 of the column height. This is a typical assumption as adopted by most researchers. However, lateral geometrical imperfection for rafter is given by Eq. (1) in accordance with Greiner et al. [24].

$$y(x) = \frac{L}{1000}\sin\left(\frac{\pi x}{L}\right). \tag{1}$$

It should be pointed out that the residual stresses are assumed to be minimal for all structural members since they comprise of hollow sections that are fabricated using weld. Meanwhile, the creep effect and the cooling phase of the portal frame are argued in a latter section; however they are generally outside the scope of this research.

Three cases of fire are considered in the current study. The first case, designated as fire case (1), is that the fire load affects all the structural elements of the frame indicating that the two columns and the rafter are exposed to fire. In the second case, designated as fire case (2), the fire load is applied to one column and the rafter of the frame while the other column is fully protected against fire. The third case, designated as fire case (3), assumes that the rafter only is exposed to fire while the two columns are fully fire protected. It should be pointed out that the outer surfaces of the portal frame are considered at ambient temperature and not exposed to fire. Fig. 7 illustrates the three subject cases of fire conditions and the surfaces of the cross-sections exposed to fire.

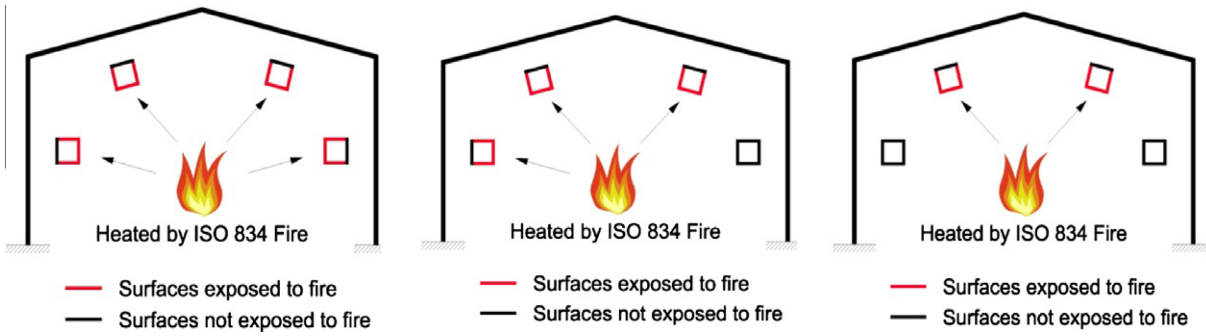

Figure 7 Simulation of fire cases.

In conjunction with the fire cases mentioned above, three inclination angles of the rafter α are studied. The angle values varies from $\alpha = 0°$ for horizontal rafter, to sharp inclination angle of $\alpha = 30°$ passing through a reasonable inclination angle of $\alpha = 11°$.

6. Results of the parametric study

The results of the parametric study are presented graphically in Figs. 8–37. The effect of fire cases on the axial force, end moment, and mid-span (apex) moment within the rafter of the frame are displayed in Figs. 8–16 in conjunction with different inclination angles α. Meanwhile, Figs. 17–22 present these effects on the apex (mid-span) deflection and horizontal displacement at the frame corners. Also, Figs. 23–28 correlate the axial force and end moments of the columns against temperature for the studied cases. Furthermore, the maximum stresses of columns and rafter at different locations are obtainable in Figs. 29–37.

6.1. Axial force in rafter

Axial forces within the rafter vary markedly with the associated fire case as shown in Figs. 8–10. It is obvious from the figures that the axial force increases slightly till approximately 400 °C where steel's yield stress begins to reduce. After that point, the axial force grows up rapidly reaching its peak value at about 520 °C, 500 °C and 680 °C for the three fire cases. The peak axial force in the rafter for fire cases (2) and (3) increases by 22% and 72% with respect to that in fire case (1). It is of interest to note that for fire cases (1) and (2), the peak axial forces are associated with yielding the columns at both ends. However, for fire case (3) and due to the rigidity of the columns, the rafter can sustain much axial force. After yielding, the axial force reduces rapidly due to yielding of the rafter's bottom flange. Hence, the axial force is fluctuating till failure that occurs at about 760 °C. Similar finding is noticeable for cases of $\alpha = 11°$ and $\alpha = 30°$. It seems that the angle of inclination affects the values of initial and peak axial force. Increasing the inclination angle from 0° to 30° leads to an increase of about 91% for the initial axial force, 40% for the

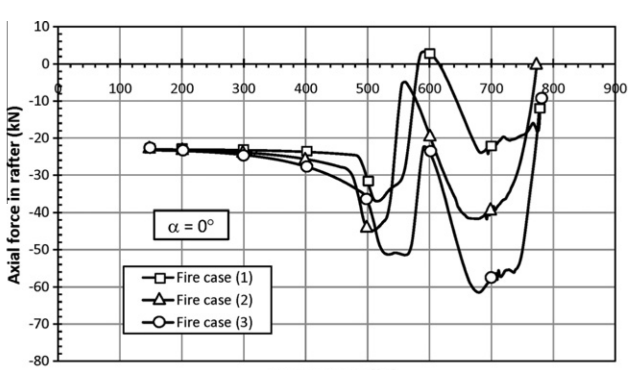

Figure 8 Developed axial force in rafter for different fire cases and for $\alpha = 0°$.

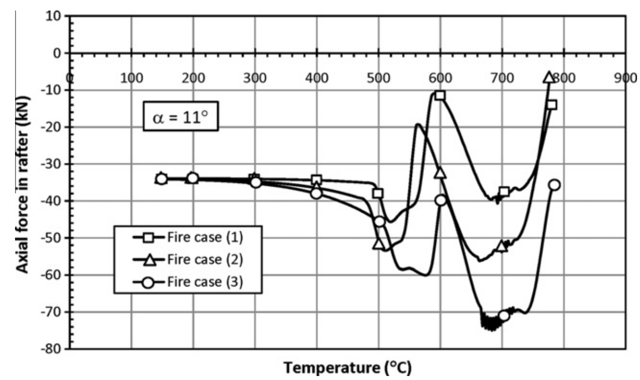

Figure 9 Developed axial force in rafter for different fire cases and for $\alpha = 11°$.

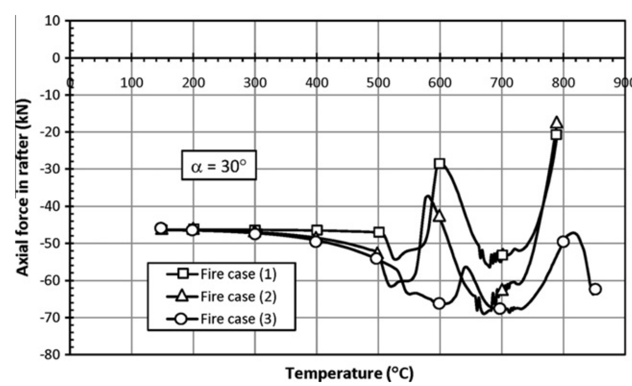

Figure 10 Developed axial force in rafter for different fire cases and for $\alpha = 30°$.

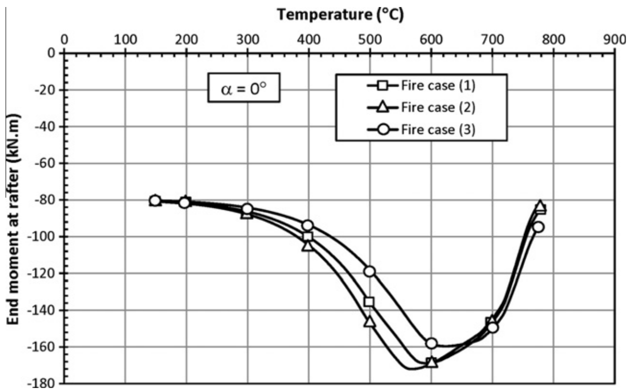

Figure 11 Developed end moments in rafter for different fire cases and for $\alpha = 0°$.

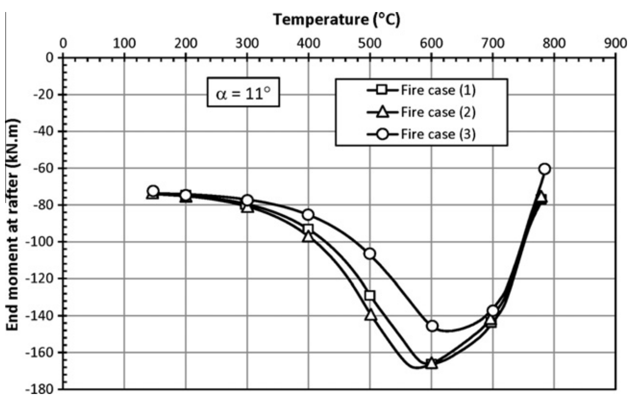

Figure 12 Developed end moments in rafter for different fire cases and for $\alpha = 11°$.

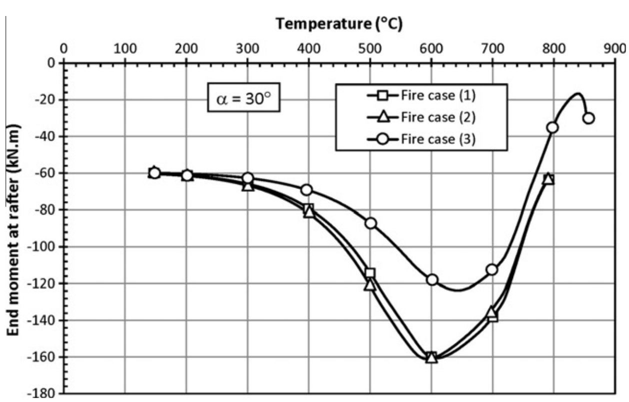

Figure 13 Developed end moments in rafter for different fire cases and for $\alpha = 30°$.

peak axial force in fire cases (1) and (2) and 10% in fire case (3).

6.2. Bending moments in rafter

6.2.1. End moments

Figs. 11–13 indicate that heating the rafter leads to increasing in the end moments due to *P*–*Δ* effects of the rafter's axial

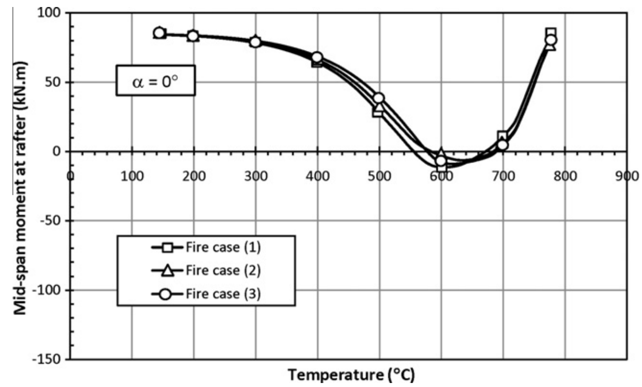

Figure 14 Developed rafter's mid-span moment for different fire cases and for $\alpha = 0°$.

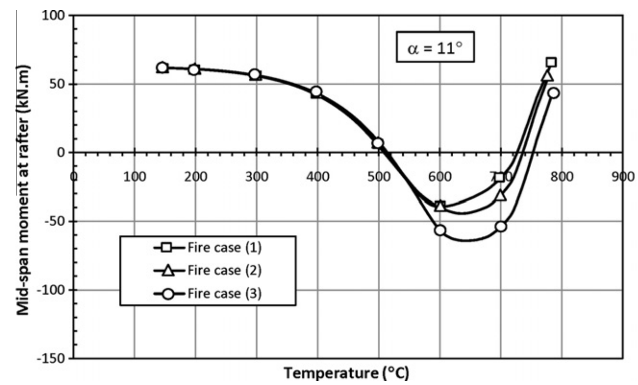

Figure 15 Developed rafter's apex moment for different fire cases and for $\alpha = 11°$.

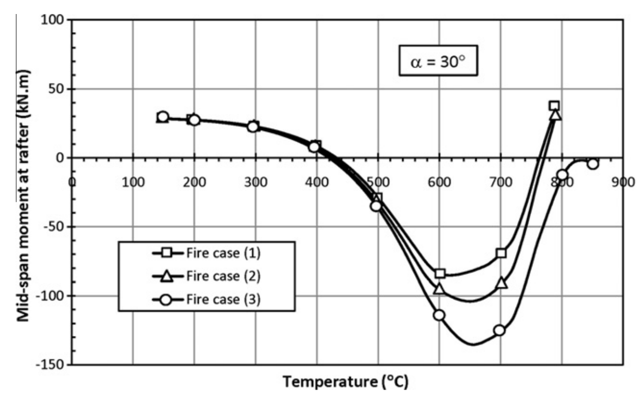

Figure 16 Developed rafter's apex moment for different fire cases and for $\alpha = 30°$.

force. After yielding of the bottom flange, the axial force in the rafter is substantially reduced, and the end moments drop accordingly. Moreover, it is noticeable that the peak end moments are comparable for fire cases (1) and (2) and reach its peak values at 600 °C. On the other hand, the values of end moments are reduced significantly for fire case (3) by increasing the inclination angle.

6.2.2. Mid-span moments

Figs. 14–16 depict the developing of the mid-span moments against temperature. It is evident from the figures that

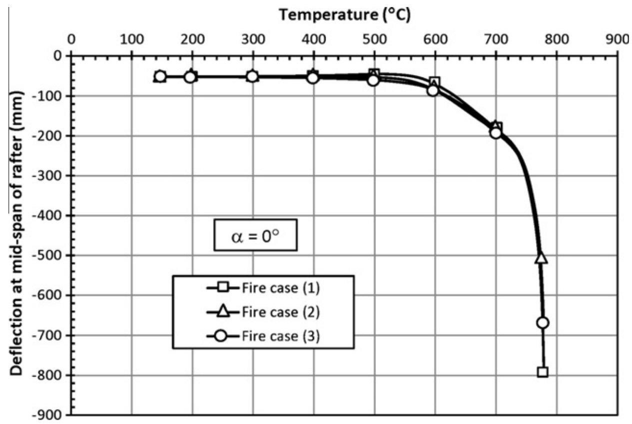

Figure 17 Developed rafter's mid-span deflection for different fire cases and for $\alpha = 0°$.

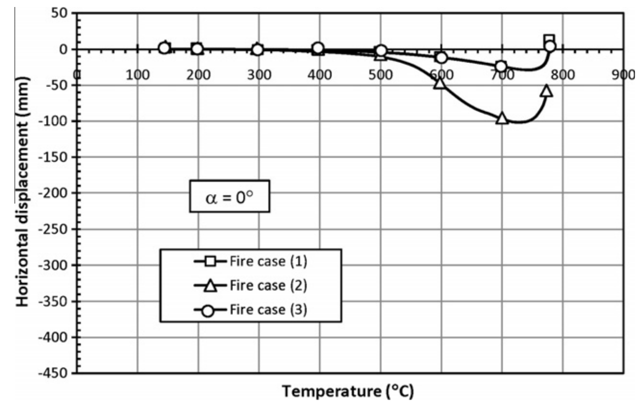

Figure 20 Developed horizontal displacement at the frame corner for different fire cases and $\alpha = 0°$.

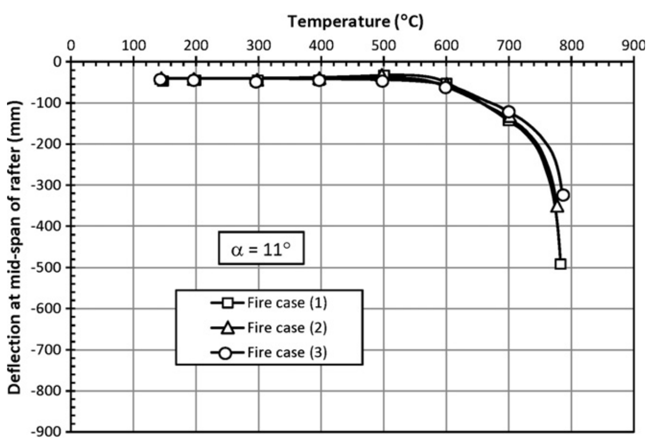

Figure 18 Developed rafter's apex deflection for different fire cases and for $\alpha = 11°$.

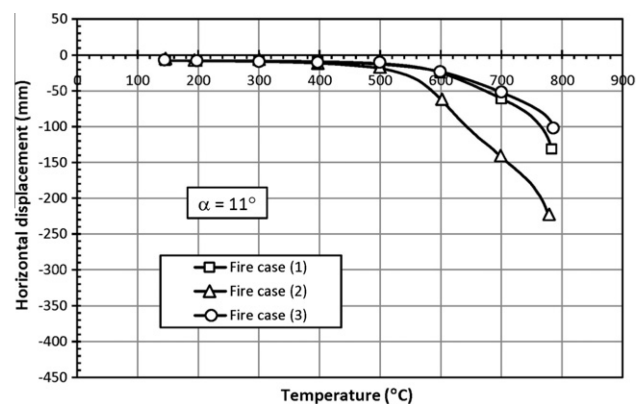

Figure 21 Developed horizontal displacement at the frame corner for different fire cases and $\alpha = 11°$.

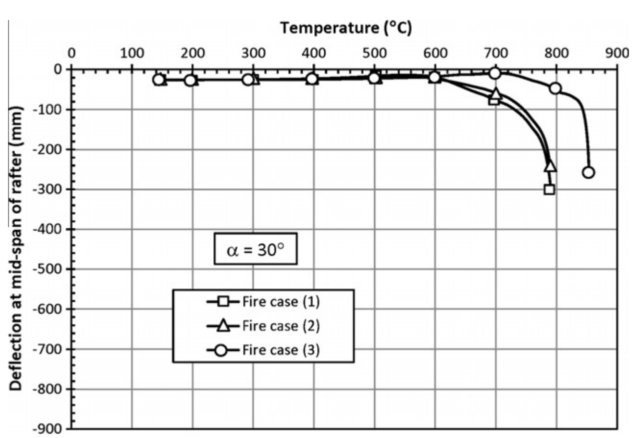

Figure 19 Developed rafter's apex deflection for different fire cases and for $\alpha = 30°$.

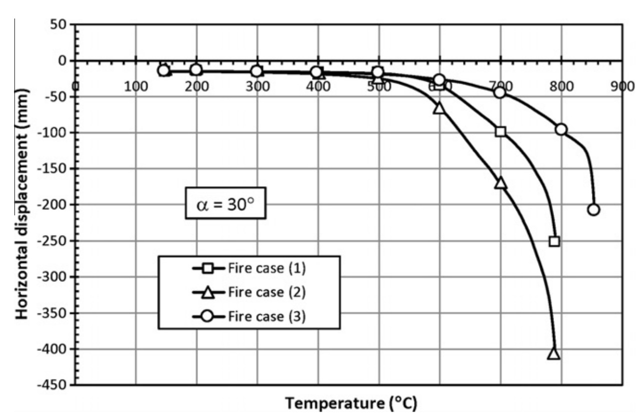

Figure 22 Developed horizontal displacement at the frame corner for different fire cases and $\alpha = 30°$.

throughout the fire duration the total magnitude of average bending moments at the rafter ends and the mid-span moment are slightly different as compared to the expected bending moments at ambient temperature ($wl^2/8$). The difference is about 7%. This may be due to the effect of geometrical imperfections taken in this study.

From monitoring the development of mid-span moments, the variation seems to be similar regardless the fire case for

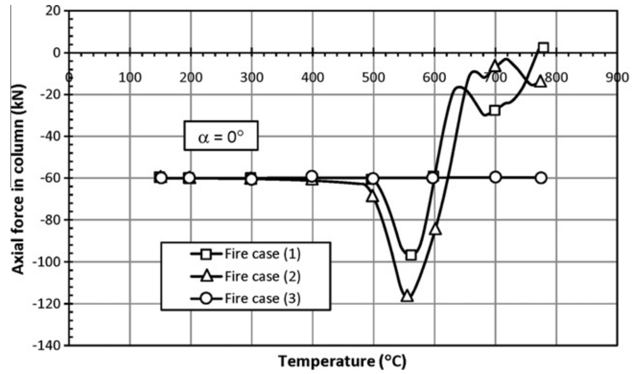

Figure 23 Developed column's axial force for different fire cases and for $\alpha = 0°$.

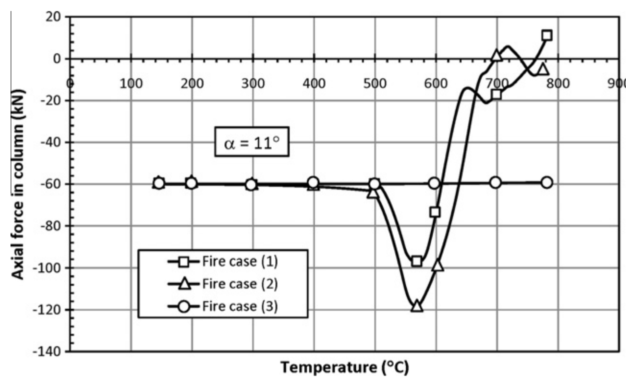

Figure 24 Developed column's axial force for different fire cases and for $\alpha = 11°$.

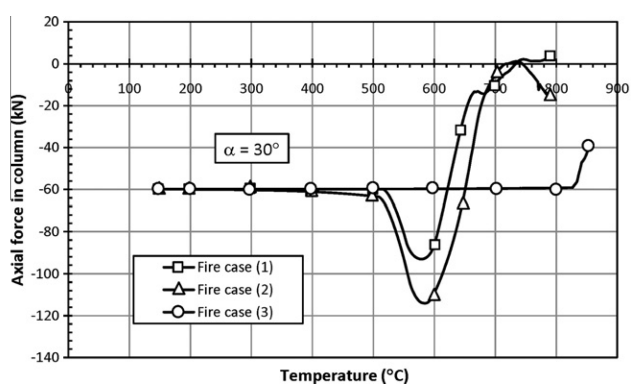

Figure 25 Developed column's axial force for different fire cases and for $\alpha = 30°$.

horizontal rafters. However, the variation is noticeable for pitched rafters where the increase in the inclination angle results in increasing the effect of fire condition on mid-span moments.

6.3. Apex deflection in rafter

The apex deflections of the analyzed frames are plotted in Figs. 17–19. From general prospective, the mid-span deflections are comparable regardless the fire case; however, the inclination

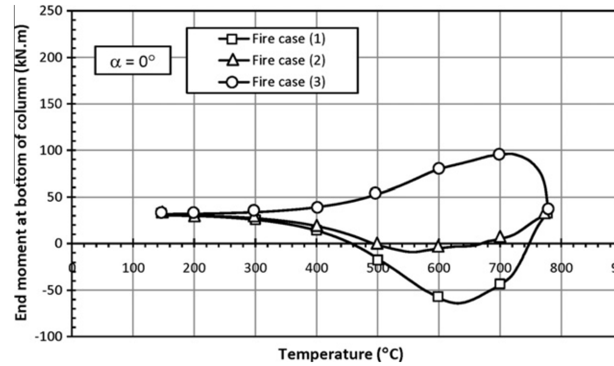

Figure 26 Developed moments at column's base for different fire cases pro $\alpha = 0°$.

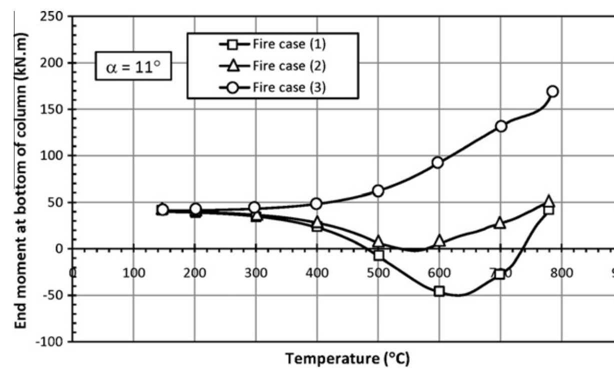

Figure 27 Developed moments at column's base for different fire cases pro $\alpha = 11°$.

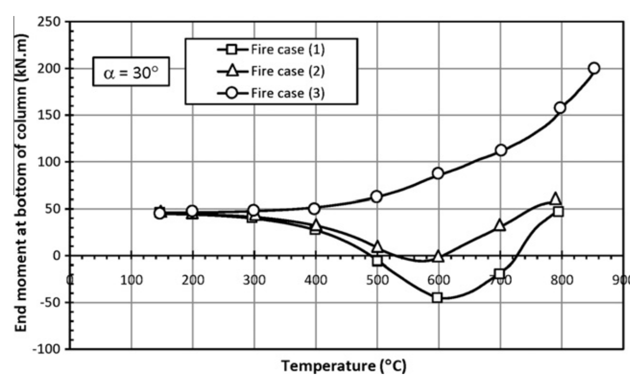

Figure 28 Developed moments at column's base for different fire cases pro $\alpha = 30°$.

angle to have pronounced effect up till a temperature of approximately 500 °C. Subsequently, the deflection increases drastically for different fire conditions. It is interesting to note that in this situation the frame starts to become geometrically unstable. The large deflection observed for horizontal frames simulates mostly the formation of plastic hinge at that location. The results indicate that inclination angle affects markedly the apex deflection. This may be due to the frame geometry which changes the failure mechanism of horizontal frames from beam mechanism to combined mechanism for pitched roof frames.

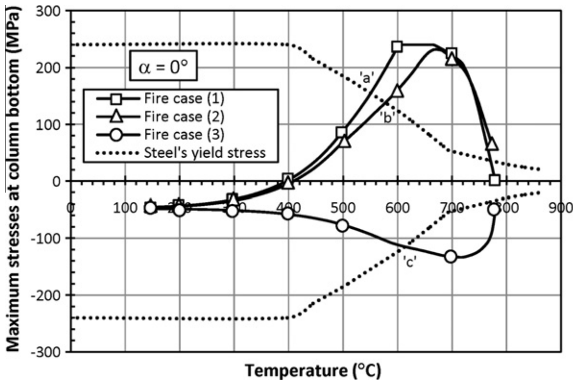

Figure 29 Developed maximum stresses at column's base for different fire cases and for $\alpha = 0°$.

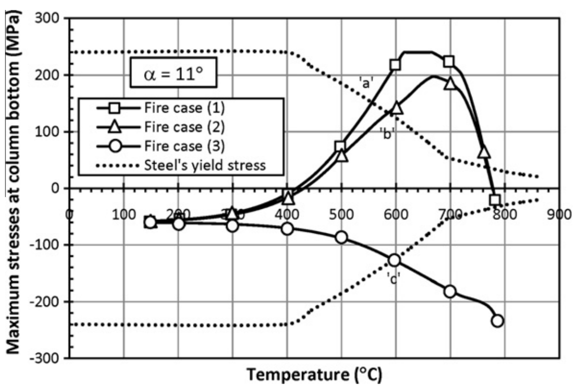

Figure 30 Developed maximum stresses at column's base for different fire cases and for $\alpha = 11°$.

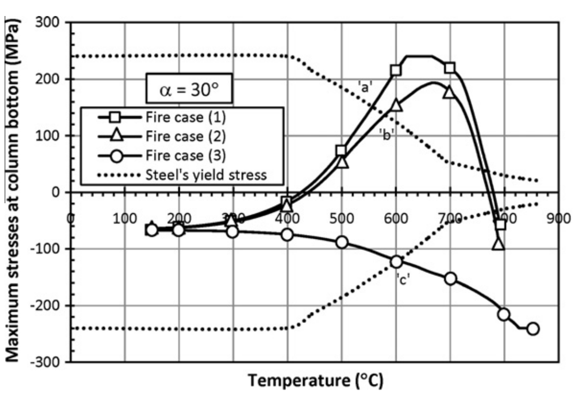

Figure 31 Developed maximum stresses at column's base for different fire cases and for $\alpha = 30$.

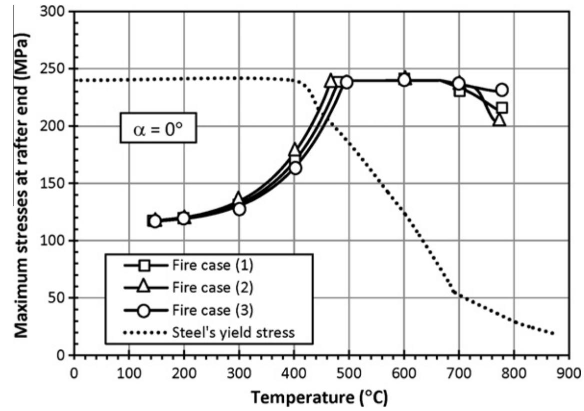

Figure 32 Developed maximum stresses at rafter's end for different fire cases and for $\alpha = 0°$.

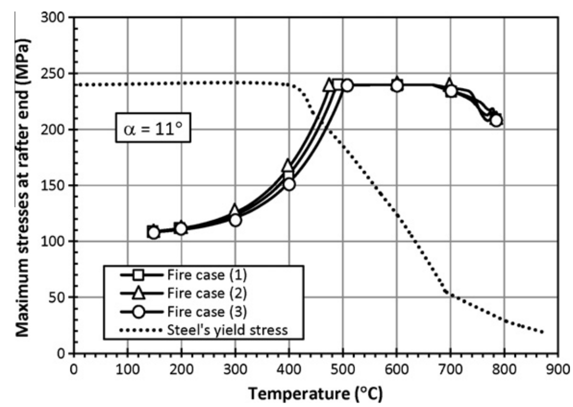

Figure 33 Developed maximum stresses at rafter's end for different fire cases and for $\alpha = 11°$.

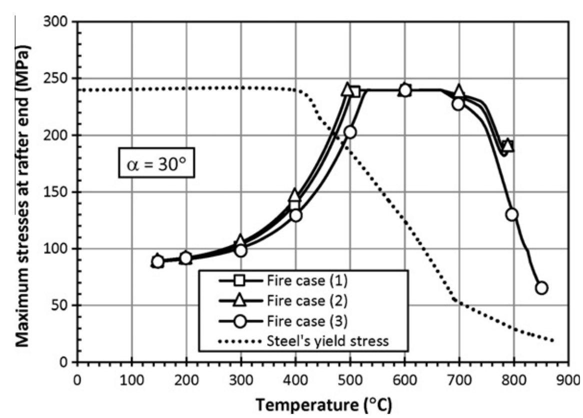

Figure 34 Developed maximum stresses at rafter's end for different fire cases and for $\alpha = 30$.

6.4. Horizontal displacement of the frame corner

The evolution of horizontal displacement at the frame corner with temperature is depicted in Figs. 20–22. For the studied fire cases, typical behavior is noticeable where initial values of horizontal displacement increases till the axial force in the rafter reaches its peak value at 500 °C. Subsequently, the displacement is set rapidly till failure in the opposite direction for frames with horizontal rafter. Different finding is set out for pitched roof frames where horizontal displacement increases rapidly till failure and no reversible displacement occurs. This may be due to the difference in failure mechanisms between horizontal and portal frames which are associated by combined mechanism as compared to the horizontal frames that are associated with beam mechanism.

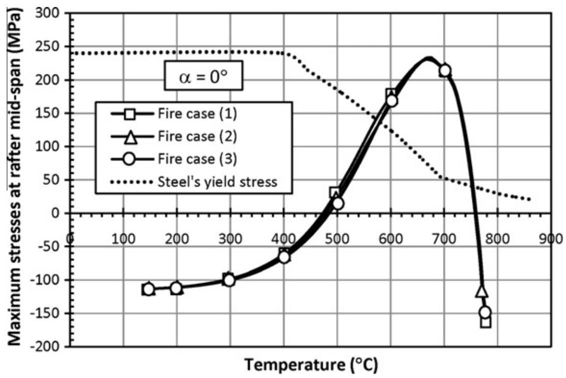

Figure 35 Developed maximum stresses at rafter's mid-span for different fire cases and for $\alpha = 0°$.

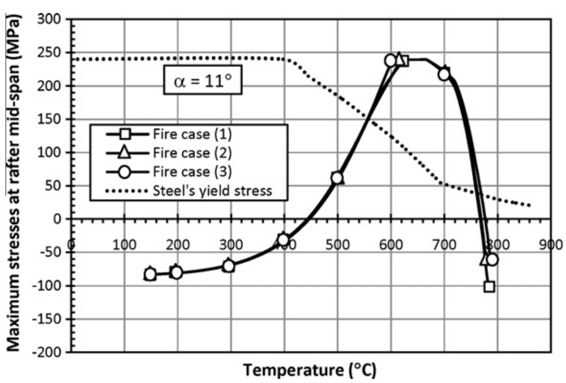

Figure 36 Developed maximum stresses at rafter's apex for different fire cases and for $\alpha = 11°$.

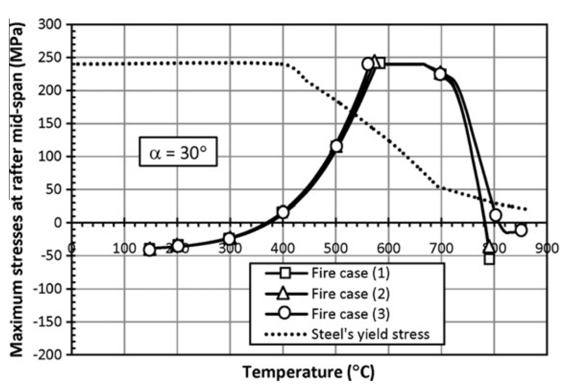

Figure 37 Developed maximum stresses at rafter's apex for different fire cases and for $\alpha = 30°$.

6.5. Axial force in columns

As shown in Figs. 23–25, axial forces within columns seem to be comparable up till 500 °C for fire cases (1) and (2). The axial force starts then to increase by increasing temperature till reaching 550 °C. After that, the column's axial force reduces rapidly till failure. Different trend is noticeable for fire case (3) where the column's axial force is constant due to the case nature. Similar observations are drawn for frames with different inclination angles.

6.6. Bending moments at bottom of columns

The variations of end moments at the bottom of columns are plotted against temperature in Figs. 26–28. The figures indicate that the end moments at the columns' bases behave comparably throughout the fire duration in fire cases (1) and (2). In such cases, the effect of the inclination angle is minimal and the plastic hinges occur. However, for fire case (3) where only the rafter is subjected to fire load, the column's bottom moments increase rapidly with temperature till failure due the increase in axial force generated in the rafter. It should be emphasizing that this observation is not pronounced for horizontal rafter where the axial force is much lesser than those of inclined rafters. Furthermore, due to reversing the axial force direction from compression to tension before failure, end moments at the column's bottom start to decrease just before failure.

6.7. Stresses at bottom of columns

The stresses developed at column's base as affected by fire temperature can be seen in Figs. 29–31. The dotted curves in the graphs represent the yield stress of steel as affected by the fire temperature. The figures clearly demonstrate that the stresses at column's bottom are remarkable due to column bending moments as previously discussed. From general prospective, as the inside flange of the column is under tension while the outside flange is under compression, the column is bowing out. In addition, results clearly indicate that the column's cross-section yields faster for fire case (1) as denoted by point 'a' in the graphs rather than the other two fire cases represented by points 'b' and 'c'. This is due to the nature of fire case which exhibits combined failure mechanism for all angles inclination.

6.8. Stresses in rafter

6.8.1. Stresses at the end of rafter

The stresses developed in all studied cases are shown in Fig. 32 and 33. Again, the dotted curves in the graphs represent the yield stress of steel as affected by temperature. It is obvious that the stresses reach the yield values at about 450 °C forming plastic hinges at the corners. It is also noticeable that the rafter connected to columns not exposed to fire (case 3) may yield at slightly higher temperature than the other fire cases. Temperature associated with yielding increases by 5%, 12% and 4% for inclination angles of 0°, 11° and 30°, respectively, as compared to case (2).

6.8.2. Stresses at the mid-span (apex) of rafter

As expected, the tensile stresses at the mid-span of the rafter are comparable for all studied frames as shown in Figs. 35–37. It is of interest to note herein that the plastic hinge occurs at the rafter's mid-span (apex) at similar temperatures for different fire conditions. Meanwhile, increasing the inclination angle α surrenders slightly less temperature with respect to the stresses at the apex. For example, the increase in the inclination angle from 0° up to 30° leads to a reduction in temperature by about 8.5%.

7. Failure temperatures and failure mechanisms

The failure criterion of the analyzed portal frames was previously identified as the formation of sufficient numbers of plastic hinges to form mechanism. It was noticeable herein that the failure mechanism was changed by changing the fire condition and the rafter inclination.

The failure mechanism is changed dramatically by changing the frame geometry from horizontal to pitched roof as shown in Table 3. For horizontal frames, beam mechanism is encountered for fire cases (2) and (3) while sway mechanism is noticeable for fire case (1). However, for pitched roof frames, combined mechanisms are observed regardless the case of fire and the inclination angle. It should be explored that the failure temperatures for the studied portal frames changes on the basis of the associated failure mechanism as seen in Table 3 and Fig. 38. Generally, increasing the inclination angle slightly increases the failure temperature. For example, when the inclination angle increases from 0° to 30°, the failure temperature of the frame improves by up to 5%. Actually, this enhancement is minimal. Besides, varying the fire condition changes its contribution to the failure temperature of portal frame. Furthermore, the results show that for the same rafter's inclination angle, the failure temperature increases by 6% and 10% as the fire condition changes from fire case (1) to fire cases (2) and (3), respectively.

Based on the above argument, it seems reasonable to conclude that the effects of both rafter's inclination angle and the fire condition on the output failure temperature are minimal and hence could be disregarded in design. However, their effects on the failure mechanism are pronounced. Actually, from the safety point of view, it is very imperative for the designer to find out and hence trace the failure mechanism prior to the completion of the final design stage. Only at this point, the optimum fire protection or section capacity can be accomplished.

8. Conclusions

Based on the study reported herein, the following conclusions can be drawn:

1. A numerical investigation on the behavior of portal frames comprised of steel hollow sections under various fire conditions is presented. Finite element technique using a powerful 'SAFIR Software' is utilized. The prime concern is to determine the failure mechanisms and the associated failure temperatures for portal frames.
2. A proposed failure criterion depending on the formation of plastic hinges is clearly demonstrated and introduced as a powerful tool for assessment.
3. A comparative study between the results predicted by the proposed model and experimental data reported elsewhere is presented. The comparison shows good agreement indicating the validity of the considered failure criterion.
4. Results indicates that the generated internal forces in rafter and apex deflections are comparable regardless the fire case; however, the inclination angle has pronounced effect up to a temperature 500 °C. After this point, the generated internal forces and apex deflections vary drastically for different fire conditions. It is of great interest to note that under this circumstance the frame starts to become geometrically unstable due to the formation of plastic hinges.
5. The straining actions within columns seem to be similar up till 500 °C for fire cases (1) and (2) where at least one column is affected by fire. In such cases, the effect of the inclination angle is minimal and the plastic hinges occur. However, for fire case (3), where all columns are not suffered from fire, the column's bottom moments increase rapidly with temperature till failure due the increase in axial force generated in the rafter. This finding is not pronounced for horizontal rafter where the axial force is lesser than those of inclined rafters.
6. The stresses developed at column's base are remarkable due to columns' straining actions. Results clearly indicate that the column's cross-section yields faster for fire case (1) rather than the other two fire cases. On the other hand, the stresses at rafter's end reaches the yield values at 450 °C forming plastic hinges at the corners.
7. The stresses at the mid-span of the rafter are comparable for all studied frames. The plastic hinge occurs at the rafter's mid-span (apex) at similar temperatures for different fire conditions. Meanwhile, increasing the inclination angle α surrenders slightly less temperature with respect to the stresses at the apex.
8. From general prospective, the failure mechanisms of portal frames are significantly affected by changing the fire condition in despite of the slightly difference in failure temperatures that is limited to 10%.
9. Inclination angle of the rafter reaches its maximum effect on the failure temperatures of the subject frames at fire case (3) where the rafter is only exposed to fire. Increasing the inclination angle from 0° to 30° leads to an increase in the failure temperature by only 4%.
10. The failure mechanism is changed considerably by changing the frame geometry from horizontal to pitched roof. For horizontal frames, beam mechanism is encountered for fire cases (2) and (3) while sway mechanism is noticeable for fire case (1). However, for pitched roof frames, combined mechanisms are observed regardless the case of fire and the inclination angle.
11. Despite that slightly enhancement in failure temperatures are observed when using pitched roof frames over horizontal frames, the failure mechanisms of horizontal frames are mostly associated with beam mechanisms which are more preferable as local mechanisms as compared to the global mechanisms associated with pitched roof frames.
12. The overall findings indicate that the use of protected columns in portal frames, whether these frames are horizontal or pitched roof, to improve failure temperatures are not promising. However, it is very advisable in the area of construction to state that using protected columns may lead to local failure in the frame (beam mechanism) which can be easily repaired. Conversely, in the absence of column's protection global failure in the frame possibly will occur.
13. Based on the above argument, it seems reasonable to conclude that the effects of both rafter's inclination angle and the fire condition on the output failure

Table 3 Failure temperatures and corresponding failure mechanisms.

Frame type	Inclination angle, α	Fire case	Failure temperature (°)	Failure mechanism	
Horizontal portal frame	α = 0°	1	550	Sway mechanism	
		2	577	Beam mechanism	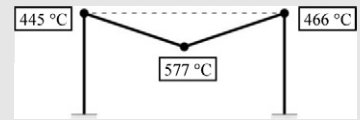
		3	577	Beam mechanism	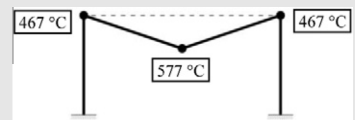
Pitched roof portal frame	α = 11°	1	556	Sway mechanism	
		2	582	Combined mechanism (3)	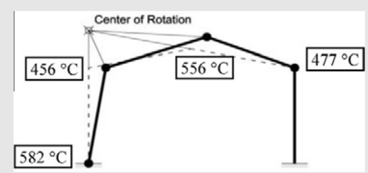
		3	591	Combined mechanism (1)	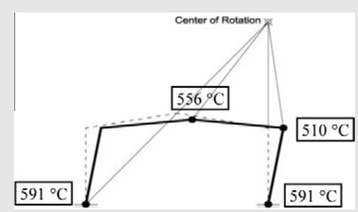
Pitched roof portal frame	α = 30°	1	556	Combined mechanism (2)	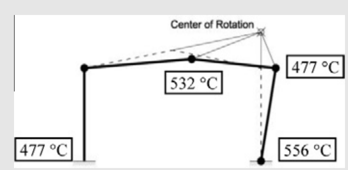
		2	577	Combined mechanism (3)	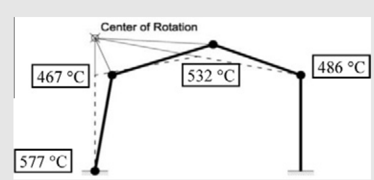
		3	599	Combined mechanism (1)	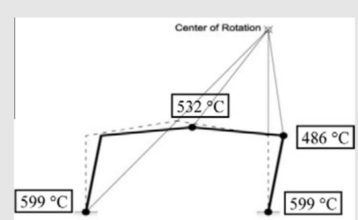

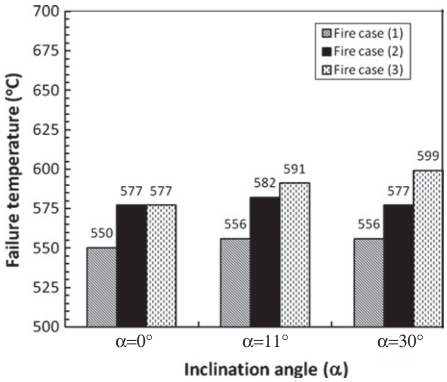

Figure 38 Effect of inclination angle on the failure temperatures for different fire cases.

temperature are minimal and hence could be disregarded in design. However, their effects on the failure mechanism are pronounced.

14. From the safety point of view, it is very imperative for the designer to find out and hence trace the failure mechanism prior to the completion of the final design stage. Only at this point, the optimum fire protection or section capacity can be accomplished.

References

[1] A. Santiago, L. Simo~ es da Silva, P. Vila Real, M. Veljkovic, Numerical study of a steel sub-frame in fire, Computers and Structures 86 (2008) 1619–1632.
[2] L. Simo~ es da Silva, A. Santiago, D. Moore, P. Vila Real, Behavior of steel joints under fire loading, International Journal of Steel and Composite Structures 5 (6) (2005) 485–513.
[3] J.B. Schleich, J.C. Dotreppe, J.M. Franssen, Numerical simulations of fire resistance tests on steel and composite structural elements or frames, in: Proc., 1st Int. Symp., Fire Safety Sci., International Association for Fire Safety Science, Boston, 1985, pp. 311–323.
[4] H.A. Saab, D.A. Nethercot, Modeling steel frame behavior under fire conditions, Engineering Structures 13 (1991) 371–382.
[5] T. Liu, Finite-element modeling of behaviors of steel rafters and connections in fire, Journal of Constructional Steel Research 36 (3) (1996) 181–199.
[6] S. Najjar, I. Burgess, A nonlinear analysis for three-dimensional steel frames in fire conditions, Engineering Structures 18 (1) (1996) 77–89.
[7] W. Morris, J. Kirby, Computers and fire-safe structural design, in: L. Kempner Jr., C.B. Brown (Eds.), Proc. Structural Congress XV, vol. 2, ASCE, New York, 1997, pp. 518–522.
[8] M.B. Wong, Plastic frame analysis under fire conditions, Journal of Structural Engineering, ASCE 127 (3) (2001) 290–295.
[9] M.A. O'Connor, D.M. Martin, Behavior of a multistory steel-framed building subjected to fire attack, Journal of Constructional Steel Research 46 (1998) 1–3.
[10] M. El-heweity, Effect of frame action on the behavior of steel rafters exposed to fire, in: Proc., IC-SGECT '04, International Conference on Structural & Geotechnical Engineering and Construction Technology, 2004, Mansoura, Egypt.
[11] Y.S. Wong, The structural Response of Industrial Portal frame Structures in Fire, Ph.D. thesis, University of Sheffield, 2001.
[12] Y. Song, Z. Huang, I.W. Burgess, R.J. Plank, The design of pitched roof steel portal frames against fire, in: Proc., 5th Int. Conf. in Steel Structures, vol. III, 2007, pp. 728–733.
[13] Y.Z. Yin, Y.C. Wang, A numerical study of large deflection behavior of restrained steel rafters at elevated temperatures, Journal of Constructional Steel Research 60 (2004) 1029–1047.
[14] M. Rahman, J. Lim, R. Hamilton, T. Komleckci, D. Pritchard, Y. Xu, An investigation of overturning moments of portal frames at elevated temperatures, in: Proc., Int. Conf. in Application of Structural Fire Engineering, 2009 (Annex 2).
[15] J.M. Franssen, V.K.R. Kodur, J. Mason, User's Manual for SAFIR 2001 – A Computer Program for Analysis of Structures Submitted to the Fire, University of Liege, Belgium, 2000.
[16] EC3-Eurocode3: Design of steel structures. Part 1–2: General rules-structural fire design, Brussels, Belgium, 2005.
[17] ISO (International Standards Organization), ISO 834, Fire resistance tests, elements of building construction, Switzerland: International Standards Organization, 1980.
[18] M.R. Horne, L.G. MORRIS, Plastic Design of Low-rise Frames, Granada Publishing Limited, 1981.
[19] J. Heyman, Plastic Design of Structures, vols. 1 and 2, Cambridge University Press, 1969.
[20] M.R. Horne, Plastic Theory of Structures, Pergamon Press Ltd., 1979.
[21] A. Rubert, P. Schaumann, Structural steel and plane frame assemblies under fire action, Fire Safety Journal 10 (3) (1986) 173–184.
[22] ECP-LRFD, Load and resistance factor design. 205-MD No. 359-2007. Permanent committee for the Code of Practice for Steel Construction and Bridges, 2009.
[23] R. Welsh, 2-D Analysis of Composite Steel-Concrete Rafters in Fire, Department of Civil Engineering, University of Canterbury, Christchurch, New Zealand, 2001.
[24] R. Greiner, G. Salzgeber, R. Ofner, New lateral–torsional buckling curves vLT-numerical simulations and design formulae, Document ECCS TC8-Report 30, 2000 (rev).